


Article

Modeling of a Combined Kalina and Organic Rankine Cycle System for Waste Heat Recovery from Biogas Engine

Cem Öksel and Ali Koç * 

Mechanical Engineering Department, Faculty of Engineering and Natural Sciences, Iskenderun Technical University, 31200 Iskenderun, Turkey; cemoksel.mf15@iste.edu.tr

* Correspondence: ali.koc@iste.edu.tr

Abstract: Converting waste heat into electricity has captured the interest of scientists for years because of its enormous potential to improve energy efficiency and to lessen environmental impacts. While there are numerous applications to recover lost energy, they are often not efficient or cheap enough to make a real-world impact. The aim of this study is to develop a heat recovery system for the waste recycling factory operating in Hatay, Turkey. We combined the Kalina Cycle (KC) with the Organic Rankine Cycle (ORC) to extract exhaust gas and jacket water waste heat from a combined heat and power engine. An ammonia–water mixture was selected as the working fluid in KC, while R123, R236ea and R124 were chosen and tested for the ORC. The selection of working fluids was made based on certain environmental impacts such as global warming or ozone depletion potential, without further exploring other working fluid options, which could be considered a limitation of this study. The optimal values of KC parameters, including mass fraction, turbine inlet pressure and inlet temperature, were found to be 90%, 430 °C and 90 bar, respectively. The KC was then combined with the ORC using three different working fluids, among which R123 yielded the best results. The net power, exergy and thermal efficiency of the combined cycle were calculated as 211.03 kW, 52.83% and 26.50%, respectively, while the payback period was estimated to be 4.2 years. It should be noted that the applicability domain of the obtained results is limited to the climate conditions studied here. We concluded that the combination of the KC and ORC can be efficiently used for the recovery of waste heat energy.

Keywords: waste heat recovery; heat integration; energy efficiency; Kalina Cycle; Organic Rankine Cycle; cogeneration; CHP engine



Citation: Öksel, C.; Koç, A. Modeling of a Combined Kalina and Organic Rankine Cycle System for Waste Heat Recovery from Biogas Engine.

Sustainability **2022**, *14*, 7135. <https://doi.org/10.3390/su14127135>

Academic Editors: Poh Seng Lee and Fahid Riaz

Received: 5 April 2022

Accepted: 26 May 2022

Published: 10 June 2022

Publisher's Note: MDPI stays neutral with regard to jurisdictional claims in published maps and institutional affiliations.



Copyright: © 2022 by the authors. Licensee MDPI, Basel, Switzerland. This article is an open access article distributed under the terms and conditions of the Creative Commons Attribution (CC BY) license (<https://creativecommons.org/licenses/by/4.0/>).

1. Introduction

Rapid economic development and industrialization has led to a growing demand for energy and heat consumption, resulting in the release of a huge amount of unused heat (so-called waste heat) into the atmosphere. About one-third of most fossil fuels is discharged into the atmosphere through exhaust gas, resulting in a large amount of heat being unused [1]. For example, only a limited amount of heat is put into practical use in energy-intensive industries such as iron, steel, cement and glass, with the remaining part being released into the surrounding environment by means of flue gases or cooling water. Therefore, energy recovery from waste heat and the need to tackle the problem of underused resources have attracted significant attention.

Waste heat recovery systems convert unused heat into an extra energy source that would otherwise be released into the atmosphere [2]. Apart from being the most economical source of energy, it also provides additional benefits by minimizing greenhouse gas emissions and lessening environmental impacts. In particular, a significant amount of waste heat can be recovered with the use of economizers or recuperators in a wide range of industrial facilities that involve conventional heating equipment such as steam-boilers and furnaces [3]. In addition to exhaust gas turbine and thermoelectric generation systems,

thermodynamic cycles such as the Rankine Cycle (RC) or Kalina Cycle (KC) are commonly used for heat recovery from industrial processes. The KC, proposed in the 1980s, uses different compositions of ammonia and water mixture for the extraction of useful work from the heat source [4]. There are numerous studies in the literature focusing on the composition optimization of the binary mixture of ammonia and water for KC [5]. There are also KC systems that use the combination of ammonia and non-water solutions as mixed working fluids [6]. A competing waste recovery system is the Organic Rankine Cycle (ORC), which uses pure organic fluids to convert heat resources into power. While KC systems have the advantage of high thermal efficiency, the ORC systems are well-suited for low-temperature applications [7]. The combination of the KC and ORC systems can also be used for the recovery of waste heat in an effective and economical manner [8,9].

Biogas production from domestic and animal wastes is increasing around the world. Moreover, the most common electricity production for these biogas power plants is CHP engines. However, as can be seen in the literature [10–17], recovering the waste heat of the CHP engines is important due to their lower efficiency (between 30% and 40%). Therefore, the main focus of the studies in the literature is recovering the waste heat of a CHP engine by assisting simple ORC or KC. However, CHP engines have low temperature waste heat (jacket water) together with high temperature waste heat. Therefore, especially for the high temperature waste heat recovering processes, integrating only a sole sub-cycle into the CHP engines will not be enough to recover the desired amount of waste heat. In this context, the present study deals with integrating ORC and KC to obtain a combined cycle for recovering the highest amount of heat. In addition to designing a combined cycle for CHP engines, the main novelty of the present study is evaluating the performance, thermodynamic, energy and environmental aspects of the designed combined cycle to be able to reveal the best performing and most profitable design for manufacturers and investors.

Here, we investigated the recovery of waste heat (at 450 °C, 2 kg/s) from the exhaust gas of a waste recycling factory operating in Hatay, Turkey. We combined KC and ORC with jacket water to provide an economical and efficient way of recovering waste heat from a combined heat and power (CHP) engine. To the best of our knowledge, this is the first time of combining jacket water with the subsystem of KC–ORC using multi-component working fluids. For ORC, three different working fluids (R123, R236ea and R124) were selected based on several parameters such as Global Warming Potential (GWP) and Ozone Depletion Potential (ODP) and compared in terms of cycle efficiency. Similarly, three different compositions of ammonia–water mixture (70:30, 80:20 or 90:10 wt%) were tested for KC. Different ranges of turbine inlet temperature and turbine inlet pressure were also investigated for both KC and ORC. In all cases, the optimization objective was to maximize net power, energy efficiency and exergy efficiency. The simulation software EBSILON Professional was used for thermodynamic calculations. Techno-economic evaluation was carried out to estimate the operating costs and payback period. A workflow diagram visually representing the steps followed in this study is provided in Figure 1.

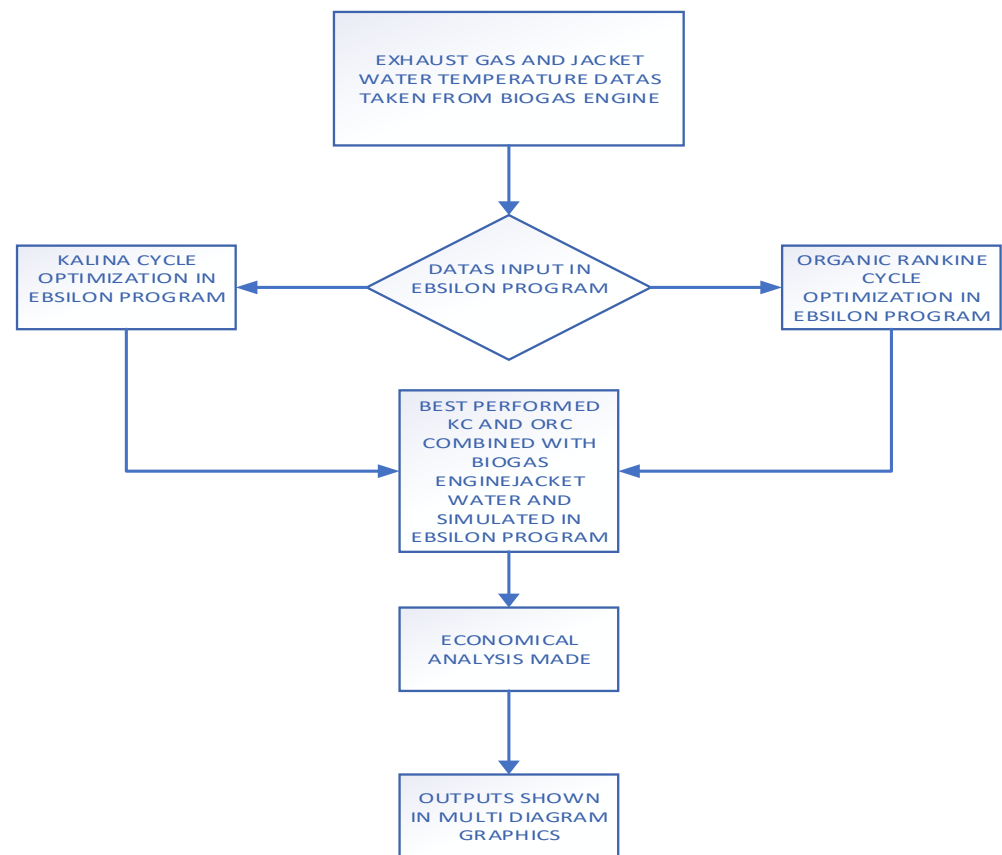


Figure 1. Flowchart visually representing the steps followed in this study.

2. System Description

2.1. CHP Engine

Waste heat recovery analysis was carried out on the depleted gas of two biogas-fuelled, eight-cylinder turbocharged engines located in a waste recycling factory in Hatay, Turkey. Both exhaust gas and jacket water waste heat were recovered to be used for indoor (e.g., local homes or greenhouse) heating. The electricity generation capacity of each CHP engine was 600 kW (two engines totalling 1200 kW). The hot exhaust gas of the CHP engine passes through a turbine where it expands to lower pressure to generate electricity and then exits to the atmosphere as by-products of combustion. The ideal working conditions of a CHP Engine are given in Table 1.

The temperature of the exhaust gas varies according to the season and the ambient temperature. In the system, the temperature of the exhaust gas is 450 °C. The mass flow rate of the depleted exhaust gas was calculated as 2 kg/s.

2.2. Combined KC and ORC

In this study, a combination of the KC and ORC systems with Heat Exchanger (HEX) is designed to improve the conversion efficiency of lost heat (from the CHP engine) to electricity. Heat exchangers are also added to the system to heat the jacket water of the engine for residential usage.

After the turbine and before the condenser of the KC, ORC with HEX was added to increase the efficiency of the system. Waste heat of the exhaust gas from the engine was recovered to generate electricity, while cooling water of the CHP engine was recovered to heat water (Figure 2). The temperature-entropy (T-s) diagram of the combined system is shown in Figure 3.

Table 1. Current working conditions of CHP engine.

Parameter	Value	Unit
$T_{jacketw,in}$	70	°C
$T_{jacketw,out}$	86	°C
$\eta_{pump_{ORC}}$	80	%
$\eta_{pump_{KC}}$	80	%
$\eta_{turbine_{ORC}}$	82	%
$\eta_{turbine_{KC}}$	82	%
$T_{coldw,in}$	20	°C
$T_{KC;exg,in}$	450	°C
$T_{KC;exg,out}$	120	°C
$P_{KC;tur,in}$	90	Bar
$P_{KC;tur,out}$	10.5	Bar
$P_{ORCC,R123;tur,in}$	35	Bar
$P_{ORCC,R123;tur,out}$	1	Bar
$P_{ORCC,R124;tur,in}$	35	Bar
$P_{ORCC,R124;tur,out}$	4	Bar
$P_{ORCC,R236;tur,in}$	33	Bar
$P_{ORCC,R236;tur,out}$	2	Bar
MPC	40.6	%
EPC	39.3	%
TPC	37.2	%
MEP	600	kWe
NOE	2	piece
$\dot{m}_{exhaust}$	2	Kg/s
$T_{exhaust,out}$	450	°C

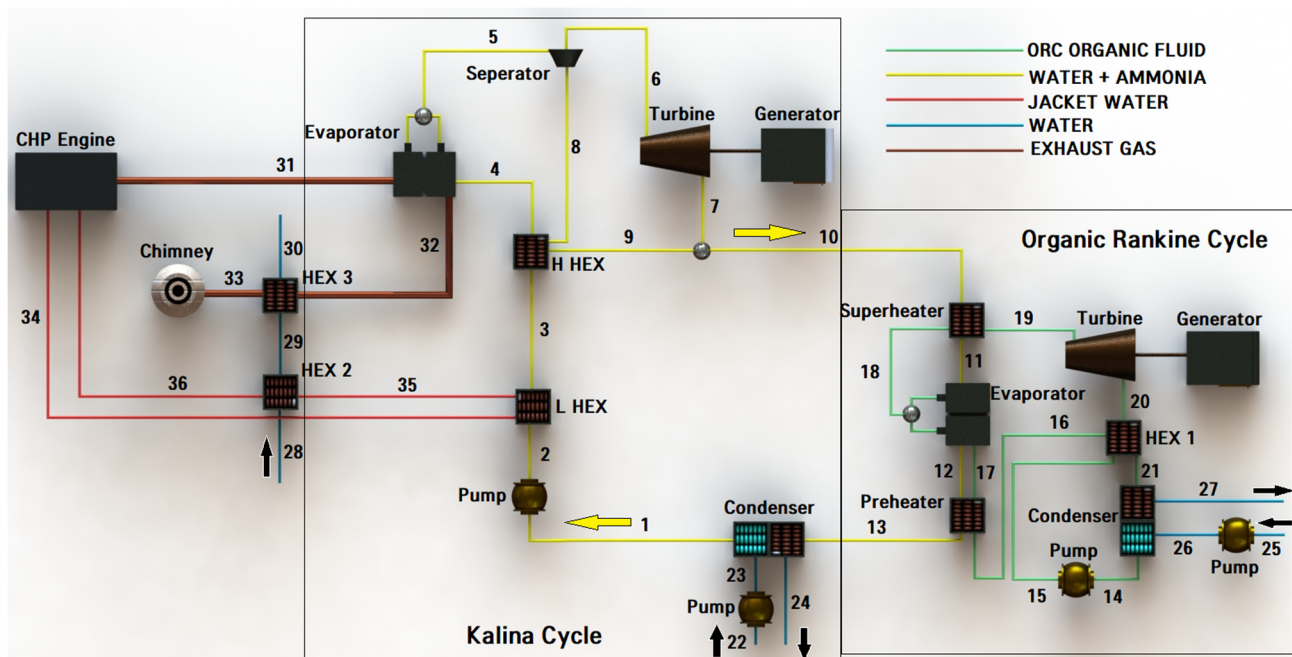


Figure 2. Combined cogeneration cycle including KC and ORC for recovering waste heat of exhaust gas and jacket water of the engine (pipes 1–13 KC, pipes 14–21 ORC, pipes 22–24 KC cooling water, pipes 25–27 ORC cooling water, pipes 28–30 water heating, pipes 31–33 flue gas and pipes 34–36 jacket water).

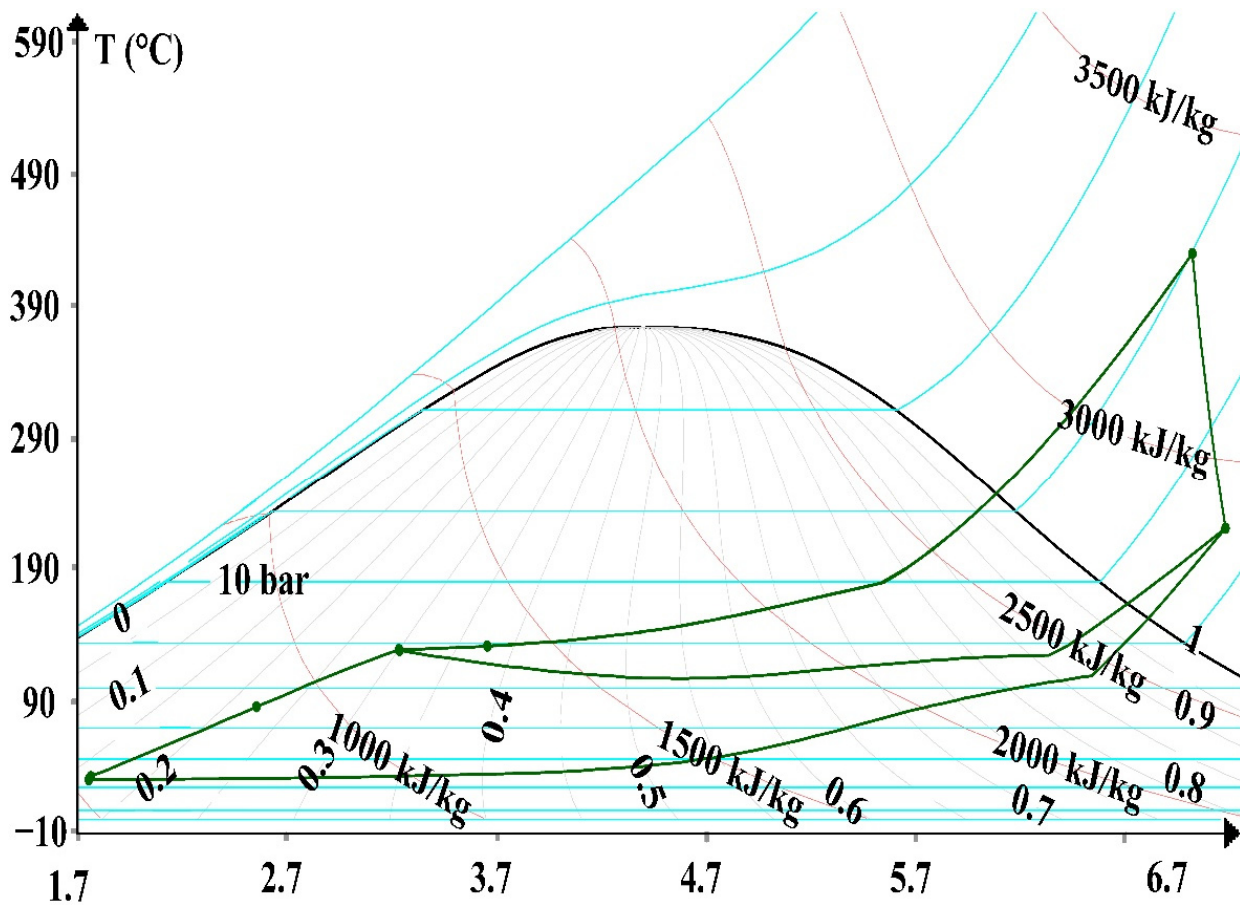


Figure 3. Temperature-entropy (T-s) diagram of the combined system (the blue lines indicate constant pressure and purple lines indicate constant enthalpy).

The KC is a thermodynamic cycle that uses working fluids of at least two different kinds to convert heat energy into mechanical power [18]. To extend thermodynamic recycling and thermodynamic performance, the ratio between these components can vary in different sections of the system [19]. For example, the use of a binary working fluid consisting of 86% ammonia and 14% water showed superior energy conversion performance in power stations when compared to traditional RC [20].

KC systems can be applied in a variety of ways, depending on the type of heat source [21]. KC can use heat sources at low temperatures as well as geothermal sources, renewable energy sources and industrial waste heat [22]. The most important feature of the ammonia–water mixture used in KC is that it has a variable boiling point, environmental friendliness and cheapness [23].

The ORC has an unclear running guideline for the routine RC, but a specific spectrum of working fluid and origin of warmth. The ORC works with natural working liquids and heat sources of low temperatures over 80 °C. Meanwhile, the ordinary RC operates with steam as the working liquid and heat sources of high temperatures over 350 °C [24]. The combined heat and power motor release the framework's abundance of heat in two forms: waste heat gas and coating cooling water. For residential warming and exhaust gas deliveries to the climate, the coat cooling water is used.

An ammonia–water mixture was selected as the working fluid in KC, while three different fluids, R123, R236ea and R124, were selected for ORC. Several parameters were taken into account when selecting the ORC working fluids, such as GWP, ODP, American Society of Heating, Refrigerating and Air-Conditioning Engineers (ASHRAE) standards, critical temperature, critical pressure and destruction temperature. The characteristic

properties of R123, R124 and R236ea are shown in Table 2, while their temperature-entropy diagram is given in Figure 4.

Table 2. Characteristic properties of chosen working fluids for ORC.

Fluid	Formula	Critical Pressure (bar)	Critical Temperature (°C)	Destruction Temperature (°C)	GWP	ODP	ASHRAE
R123	CHClCF ₃	36.61	183.68	326.85	77	0.018	B
R124	CHClF ₂ CF ₃	36.20	122.00	196.85	527	0.022	A1
R236ea	CF ₃ CH ₂ CF ₂	34.20	139.29	138.85	1200	0.000	Unknown

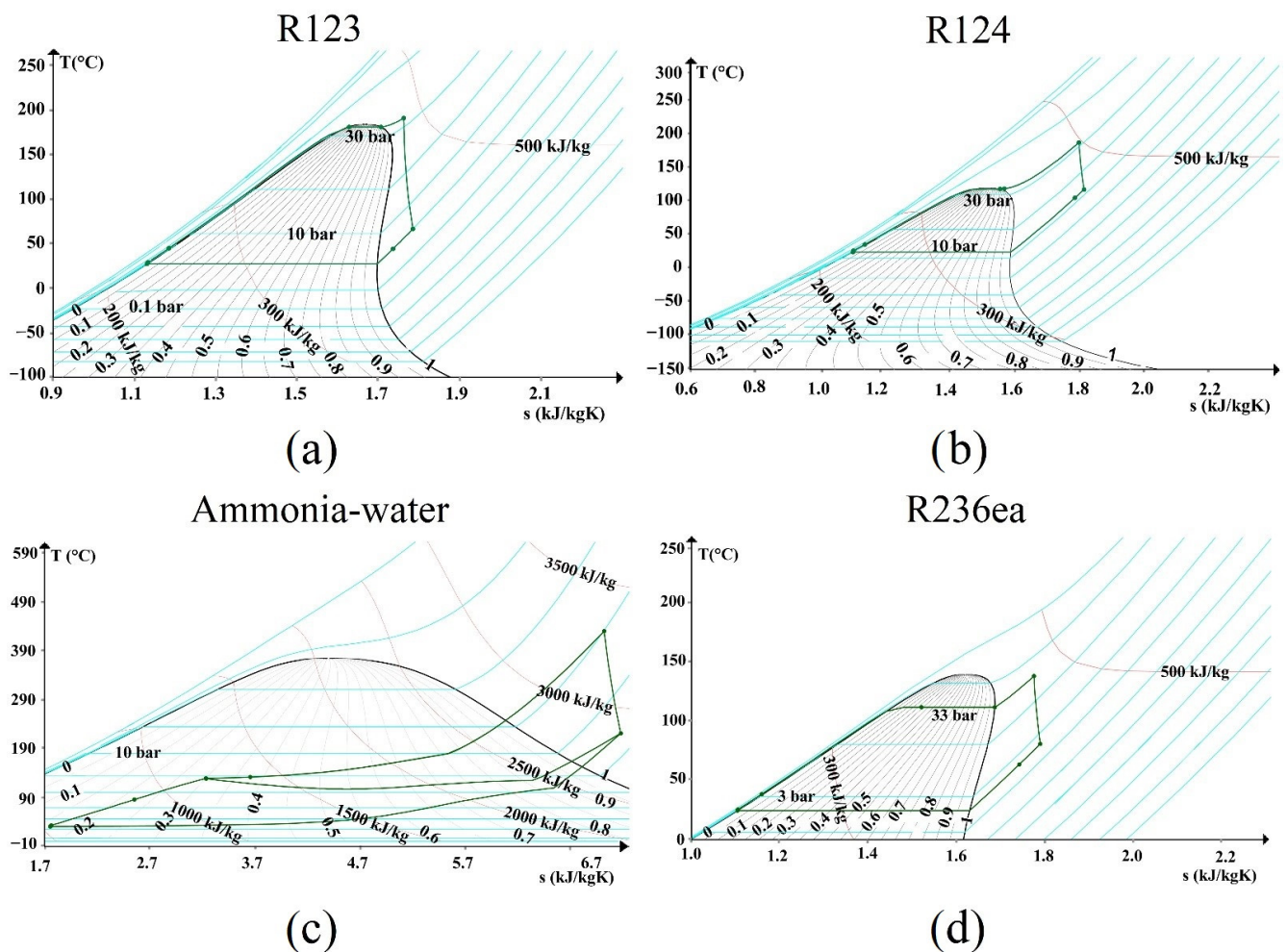


Figure 4. Temperature-Entropy diagram of working fluids (a) R123, (b) R124, (c) Ammonia-water and (d) R236ea respectively (the blue lines indicate constant pressure and purple lines indicate constant enthalpy).

In this study, the ammonia–water mixture was first sent to the evaporator unit in the cycle and brought into the vapour phase. In the meantime, the exhaust gas at 450 °C coming from the CHP system was cooled by transferring its energy to the water with the help of a HEX for residential use, sent to the chimney and released into the atmosphere.

Non-evaporated water beads in the water–ammonia mixture during vaporization were removed with a separator. The vapour phase mixture passed through the turbine where electricity was produced with the help of a generator and was directed to the mixing room. Meanwhile, the liquid fluid removed from the vapour phase mixture in the separator

passed through the high temperature HEX, gave its excess heat to the water–ammonia mixture entering the evaporator and was sent to the mixing chamber. The mixture in the mixing chamber was passed through the superheater of the ORC and gave its energy to the fluid in the ORC. Next, the mixture was sent to the condenser of the KC.

The water–ammonia mixture was condensed with the help of cooling water in the condenser. The condensed mixture was sent to the pump to be compressed to high pressure. The high-pressure mixture was sent to a low temperature heat exchanger, which was connected to the high temperature jacket water of the engine, then sent to the high temperature heat exchanger and finally, to the evaporator to complete the loop of the cycle.

In the ORC, with the help of the energy coming from the mixture in the KC, the organic liquid's temperature was increased, which was in a closed loop at the ORC until it reached the evaporation point. Then, the generated vapour expanded into the turbine to produce electrical energy through a generator. Downstream of the turbine, the vapour contributed to the HEX and condenser. The condensed fluid was then pumped into the HEX again and heated there and sent to the preheater. After the preheater, the fluid was sent to the evaporator to complete the cycle.

The jacket water of the engine was also heated with the help of the KC's low temperature HEX and cooled exhaust gas of the engine to produce hot water for residential use.

One of the characteristics that differentiates the KC from other cycles is the use of the water–ammonia mixture as the working fluid. Since the ammonia's boiling point is lower than the boiling point of water, there is a variable boiling point in the ammonia–water blend [25]. Adjusting the ammonia ratio in the ammonia–water mixture proportionally increases the power generation capacity of the system up to a certain value.

3. Mathematical Method

3.1. General Equations

This paper did not only incorporate the energetical examination of structures but also joined an exergy-based assessment of the cycles. The energy, exergy and mass examination of the combined KC and ORC was performed by utilizing the following balance formulation [26]:

$$\sum \dot{m}_{in} = \sum \dot{m}_{out} \quad (1)$$

$$\dot{Q} + \dot{W} = \sum (\dot{m}h)_{out} - \sum (\dot{m}h)_{in} \quad (2)$$

$$\dot{E}_{ex,in} = \dot{E}_{ex,out} + \dot{E}_{ex,dest} \quad (3)$$

where $\dot{E}_{ex,in}$, $\dot{E}_{ex,out}$, $\dot{E}_{ex,dest}$ refers to the exergy stream inlet, exergy stream outlet and elimination of exergy, respectively. \dot{E}_{ex} is assigned to the exergy-flow and is found by [25]:

$$\dot{E}_{ex} = \dot{m}\psi \quad (4)$$

ψ is specific exergy flow and is found by [25]:

$$\psi = (h - h_o) - T_o (s - s_o) \quad (5)$$

Work contains 100% exergy efficiency, but the heat has an exergy efficiency of less than 100%. Subsequently, to determine the exergy flow of heat ($\dot{E}_{ex,H}$), the following equation is utilized [19]:

$$\dot{E}_{ex,H} = \left(1 - \frac{T_o}{T_{HS}}\right) \dot{Q} \quad (6)$$

where T_o is the initial temperature (18 °C) and T_{HS} refers to the heat transfer surface.

The general cycle efficiency of energy and efficiency of exergy are shown as [25]:

$$\eta_{cycle} = \frac{\dot{W}_{net}}{\dot{Q}_{in}} \quad (7)$$

$$\varepsilon_{cycle} = \frac{\dot{E}_{ex;out}}{\dot{E}_{ex;in}} = \frac{\dot{W}_{net}}{\dot{E}_{ex;in}} \quad (8)$$

3.2. The Kalina Cycle

Next, the exergy and energy computations of the KC were carried out. All the heat transferred from the exhaust to the ammonia mixture of water is reached by [26]:

$$\dot{Q}_{in;KC} = \dot{m}_{exg}(h_{31} - h_{32}) = \dot{m}_{KC,mix}(h_5 - h_4) \quad (9)$$

where $\dot{m}_{KC,mix}$ is the flow rate of mass of the mixture in the KC. Net power made in the KC is found as [20]:

$$\dot{W}_{net;KC} = \dot{W}_{KC,tur} - \dot{W}_{KC,pump} \quad (10)$$

where $\dot{W}_{KC,pump}$ symbolizes the power gained from the KC turbine and $\dot{W}_{KC,tur}$ is the power of the KC pump. The KC exergy entrance from the depleted exhaust is found as [26]:

$$\dot{E}_{in;KC} = \dot{m}_{exg}(\psi_{31} - \psi_{32}) \quad (11)$$

The exergy and thermal efficiency of the solo KC system are found by [26]:

$$\eta_{KC} = \frac{\dot{W}_{net;KC}}{\dot{Q}_{in;KC}} \quad (12)$$

$$\varepsilon_{KC} = \frac{\dot{W}_{net;KC}}{\dot{E}_{in;KC}} \quad (13)$$

3.3. The Rankine Cycle

The aggregate of the heat flow from the depleted gas to liquid is calculated as [26]:

$$\dot{Q}_{in;RC} = \dot{m}_{exg}(h_{20} - h_{13}) = \dot{m}_{RC}(h_{19} - h_{15}) \quad (14)$$

where \dot{m}_{RC} in the RC is the flow rate of mass of the water. The total net power production of the RC is found as [26]:

$$\dot{W}_{net;RC} = \dot{W}_{RC,tur} - \dot{W}_{RC,pump} \quad (15)$$

where $\dot{W}_{RC,tur}$ shows the amount of power accomplished from the RC and $\dot{W}_{RC,pump}$ is the power of the RC pump. The exhaust gas exergy input to the RC is found by [26]:

$$\dot{E}_{in;RC} = \dot{m}_{exg}(\psi_{20} - \psi_{13}) \quad (16)$$

The net thermal efficiency and efficiency of exergy of the single RC are found by [26]:

$$\eta_{RC} = \frac{\dot{W}_{net;RC}}{\dot{Q}_{in;RC}} \quad (17)$$

$$\varepsilon_{RC} = \frac{\dot{W}_{net;RC}}{\dot{E}_{in;RC}} \quad (18)$$

Additionally, each KC system component was examined utilizing energy and exergy equations in addition to the overall combined system performance study. Table 3 shows the first and second law analysis formulas for the KC components.

Table 3. The first and second law analysis formulas used for the KC components.

Components	Mass and Energy	Exergy
Evaporator	$\dot{m}_{31} = \dot{m}_{32} = \dot{m}_{exg}$ $\dot{m}_4 = \dot{m}_5 = \dot{m}_{KC,mix}$ $\dot{Q}_{eva} = \dot{m}_{KC,mix}(h_5 - h_4)$	$\dot{E}_{eva,dest} = \dot{m}_{exg}(\psi_{31} - \psi_{32}) - \dot{m}_{KC,mix}(\psi_5 - \psi_4)$ $\epsilon_{eva} = \frac{\dot{m}_{KC,mix}(\psi_5 - \psi_4)}{\dot{m}_{exg}(\psi_{31} - \psi_{32})}$
Turbine	$\dot{m}_6 = \dot{m}_7 = \dot{m}_{KC,mix} - \dot{m}_8 = \dot{m}_a$ $\dot{W}_{KC,tur} = \dot{m}_a(h_6 - h_7)$ $\eta_{KC,tur} = \frac{\dot{W}_{KC,tur}}{\dot{W}_{KC,tur,s}}$	$\dot{W}_{KC,tur,rev} = \dot{m}_a(\psi_6 - \psi_7)$ $\dot{E}_{KC,tur,dest} = \dot{W}_{KC,tur,rev} - \dot{W}_{KC,tur}$ $\epsilon_t = \frac{\dot{W}_{KC,tur}}{\dot{W}_{KC,tur,rev}}$
LHEX	$\dot{m}_2 = \dot{m}_3 = \dot{m}_{34} = \dot{m}_{35} = \dot{m}_{KC}$ $\dot{Q}_{LHEX} = \dot{m}_{KC}(h_3 - h_2)$	$\dot{E}_{LHEX,dest} = \dot{m}_{34}(\psi_{34} - \psi_{35}) - \dot{m}_2(\psi_3 - \psi_2)$ $\epsilon_{LHEX} = \frac{\dot{m}_2(\psi_3 - \psi_2)}{\dot{m}_{34}(\psi_{34} - \psi_{35})}$
HHEX	$\dot{m}_3 = \dot{m}_4 = \dot{m}_{KC}$ $\dot{m}_8 = \dot{m}_9 = \dot{m}_{KC} - \dot{m}_6 = \dot{m}_s$ $\dot{Q}_{HHEX} = \dot{m}_{KC}(h_4 - h_3)$	$\dot{E}_{HHEX,dest} = \dot{m}_s(\psi_8 - \psi_9) - \dot{m}_{KC}(\psi_4 - \psi_3)$ $\epsilon_{HHEX} = \frac{\dot{m}_{KC,mix}(\psi_4 - \psi_3)}{\dot{m}_s(\psi_8 - \psi_9)}$
Condenser	$\dot{m}_{13} = \dot{m}_1 = \dot{m}_{KC,mix}$ $\dot{m}_{23} = \dot{m}_{24} = \dot{m}_{cond}$ $\dot{Q}_{KC,cond} = \dot{m}_{KC,mix}(h_{13} - h_1)$	$\dot{E}_{cond,dest} =$ $\dot{m}_{KC,mix}(\psi_{13} - \psi_1) - \dot{m}_{cond}(\psi_{24} - \psi_{23})$ $\epsilon_{KC,cond} = \frac{\dot{m}_{cond}(\psi_{24} - \psi_{23})}{\dot{m}_{KC,mix}(\psi_{13} - \psi_1)}$
Pump	$\dot{m}_1 = \dot{m}_2 = \dot{m}_{KC,mix}$ $\dot{W}_{KC,pump} = \dot{m}_{KC,mix}(h_2 - h_1)$ $\eta_{KC,pump} = \frac{\dot{W}_{KC,pump,s}}{\dot{W}_{KC,pump}}$	$\dot{W}_{KC,pump,rev} = \dot{m}_{KC,mix}(\psi_2 - \psi_1)$ $\dot{E}_{KC,pump,dest} = \dot{W}_{KC,pump} - \dot{W}_{KC,pump,rev}$ $\epsilon_{KC,pump} = \frac{\dot{W}_{KC,pump,rev}}{\dot{W}_{KC,pump}}$

The flow was considered to be in a steady-state condition throughout the analysis. The kinetic and potential energy was not taken into account. The allowed room temperature was 18 °C.

3.4. Economic Estimation

While it is crucial to expand the efficiency of heat recovery, it is equally important to evaluate economic aspects to compare energy saving benefits to the costs of waste heat recovery technologies. Therefore, we investigated the costs and economic feasibility of the proposed system. The total cost for the designed framework can be found by [27]:

$$PEC_{RC} = PEC_{prh} + PEC_{eva} + PEC_{sph} + PEC_{tur} + PEC_{Cond} + PEC_{pump} \quad (19)$$

for single RC,

$$PEC_{KC} = PEC_{tur} + PEC_{Cond} + PEC_{pump} + PEC_{LTR} + PEC_{HTR} + PEC_{eva} \quad (20)$$

for single KC, and

$$PEC_{RC-KC} = PEC_{RC} + PEC_{KC} \quad (21)$$

In KC and ORC systems, for economical analysis, investigating equipment costs is fairly crucial. In Table 4, cost equations of each equipment used in the Kalina and Rankine Cycles is shown.

Table 4. The cost equations of each equipment used in the Kalina and Rankine Cycles [27].

Rankine Cycle	
System Component	Purchased Equipment Cost (PEC)
Preheater	$130 \left(A_{prh}/0.093 \right)^{0.78}$
Evaporator	$130 \left(A_{eva}/0.093 \right)^{0.78}$
Superheater	$130 \left(A_{sph}/0.093 \right)^{0.78}$

Table 4. Cont.

Turbine	$6000 \left(\dot{W}_{RC,tur} \right)^{0.7}$
Condenser	$588 \left(A_{RC,cond} \right)^{0.8}$
Pump	$3540 \left(\dot{W}_{RC,pump} \right)^{0.7}$
Kalina Cycle	
System Component	Purchased Equipment Cost (PEC)
Turbine	$4405 \left(\dot{W}_{KC,tur} \right)^{0.7}$
Condenser	$1397 \left(A_{KC,cond} \right)^{0.89}$
Pump	$1120 \left(\dot{W}_{KC,pump} \right)^{0.8}$
LTR	$2681 \left(A_{KC,ltr} \right)^{0.59}$
HTR	$2681 \left(A_{KC,htr} \right)^{0.59}$
Evaporator	$1397 \left(A_{KC,cond} \right)^{0.89}$

Table 5 shows the economic constants that were used in the analysis.

Table 5. Constraints economical estimation [27].

Parameters	Unit	Value
Operation time in one year (n)	hour	7680
Rate of interest (i)	%	15
Factor of maintenance (ϕ)	%	6
Activity lifetime (N)	year	15
Factor of capacity (FC)	-	0.89

The operation time in one year was estimated with the extraction of the total maintenance days, which was 45 out of 365 days [27].

After calculating investment costs, the capital recovery cost (CRF) could be found by [28–30]:

$$CRF = \frac{i(1+i)^N}{(1+i)^N - 1} \quad (22)$$

Here, i and N are the interest rate and plant lifetime, respectively. The cost of the electricity produced (C_{elec}) by the k th system was also calculated in the present study by [31,32]:

$$C_{elec} = \frac{CRF \cdot PEC_k + \phi}{\dot{W}_{net,n}} \quad (23)$$

The payback period (PB_k) of e k th system was found by [27]:

$$PB_k = \frac{\log \frac{(\dot{W}_{net,n} \cdot c_{pric}) - \phi}{(\dot{W}_{net,n} \cdot c_{pric}) - \phi - (i \cdot PEC_k)}}{\log(1+i)} \quad (24)$$

where c_{pric} is the cost of the electricity in kW per hour, which is taken as 0.07 \$/kWh (1 US Dollar:13.8 Turkish Lira, TL).

4. Results and Discussion

Within the scope of this study, a combined KC and ORC system was created to regain the waste heat energy of the exhaust gas flowing at a rate of 2 kg/s, which was currently being discharged into the atmosphere at 450 °C in the heat–power combined cycle. This combined KC and ORC design was optimized using the EBSILON® Professional software program by determining the optimum ratio of the ammonia–water mixture for the KC as

well as the optimum working fluid for the ORC. In Table 6, the best performing cycle's thermodynamical results obtained using the simulation program are shown.

Table 6. State point thermodynamic results of KC and ORC.

Number	Component	Pressure bar	Temperature °C	Enthalpy kJ/kg	Mass Flow kg/s	Energy Flow kW	Density kg/m ³	Entropy kJ/kgK	Exergy kJ/kg
1	Pump KC in	10.50	30.04	372.50	0.35	131.29	640.88	1.77	203.52
2	Pump KC out	90.00	32.38	387.95	0.35	136.73	644.60	1.78	216.02
3	L HEX KC out	89.95	85.19	650.21	0.35	229.17	563.30	2.57	248.05
4	Evaporator KC in	88.95	85.18	650.21	0.35	229.17	563.14	2.57	247.91
5	Evaporator KC out	88.95	430.00	2703.95	0.35	953.02	27.18	7.03	1003.64
6	Turbine KC in	90.00	88.95	430.00	2703.95	0.35	953.02	7.03	1003.64
7	Turbine KC out	10.50	220.84	2199.76	0.35	775.31	4.47	7.18	453.64
8	Separator KC out	88.95	128.60	908.56	0.00	0.00	460.16	3.25	308.69
9	H HEX KC out	87.95	127.95	908.56	0.00	0.00	445.84	3.25	308.53
13	Condenser KC in	10.50	220.84	2199.76	0.35	775.31	4.47	7.18	453.64
31	Evaporator KC Gas in	1.20	450.00	488.24	2.00	976.48	0.57	7.98	202.11
32	Evaporator KC Gas out	1.20	120.00	126.31	2.00	252.62	1.04	7.31	34.07
23	Water Condenser KC in	2.00	15.01	63.20	15.41	973.77		0.22	0.16
24	Water Condenser KC out	1.50	25.01	105.00	15.41	1617.79	997.07	0.37	0.40
14	Pump ORC in	1.00	27.46	227.65	0.85	193.32	1457.58	1.10	0.15
15	Pump ORC out	35.10	29.23	230.57	0.85	195.79	1463.08	1.10	2.51
21	HEX ORC in	35.05	38.00	239.54	0.85	203.41	1441.01	1.13	2.96
11	Evaporator ORC in	35.05	180.17	415.30	0.85	352.66	780.89	1.58	45.66
10	Superheater ORC in	35.05	180.98	455.15	0.85	386.50	361.94	1.67	59.96
19	Turbine ORC in	35.00	185.00	469.44	0.85	398.63	288.45	1.70	65.11
20	Turbine ORC out	1.00	55.09	417.66	0.85	354.67	5.79	1.73	6.98
17	Preheater ORC out	1.00	42.61	408.70	0.85	347.05	6.04	1.70	6.10
26	Water Condenser ORC in	2.00	15.01	63.20	4.60	290.60	999.15	0.22	0.16
27	Water Condenser ORC out	1.50	23.01	96.64	4.60	444.33	997.56	0.34	0.23

4.1. The Optimization of the Single KC with Different Mass Fractions of Working Fluids

A thermodynamic study of the KC was conducted by considering the determined optimum mixing ratio and all design parameters that were assumed to be constant during the cycle analysis. Different temperatures ranging between the saturation point temperature and 430 °C were tested for the turbine inlet temperature, while three different turbine inlet pressures (70, 80 and 90 bar) were tested. The working fluid ratio was also tested for 70%, 80% and 90% to find optimum values for the system. The output of the KC was optimized in this part of the study based on the TIT, TIP and ammonia–water mixture's fraction mass ratio. The impact of the inlet temperature of the turbine, pressure and mixing ratio of the working fluid on the net power of the KC are shown in Figure 5.

The results indicate that the net power of the KC increases with the increasing of the turbine inlet temperature. The net power of the KC also increases with the increasing of the ammonia–water ratio with the increasing of the turbine inlet pressure until the saturation point and decreases after that point. The net power increases very rapidly until the decomposition in the separator is zero and increases slowly afterwards. It can be observed that a lower pressure system can produce more power in lower temperatures compared to higher pressures. The best performing KC has an optimum net power value of 168.69 kW at 430 °C, 90 bar and 90% ratio.

It has been established that the net power value increases when the mass fraction rate of the ammonia increases at various turbine inlet temperatures and turbine inlet pressures and TIPs. The lowest net power value is produced by the smallest mass fraction ratio.

In Table 7, exergy values of inlets and outlets of the equipments used in KC and ORC is shown and in Figure 6, exergy destruction ratio in terms of equipments used in KC and ORC is shown as pie chart.

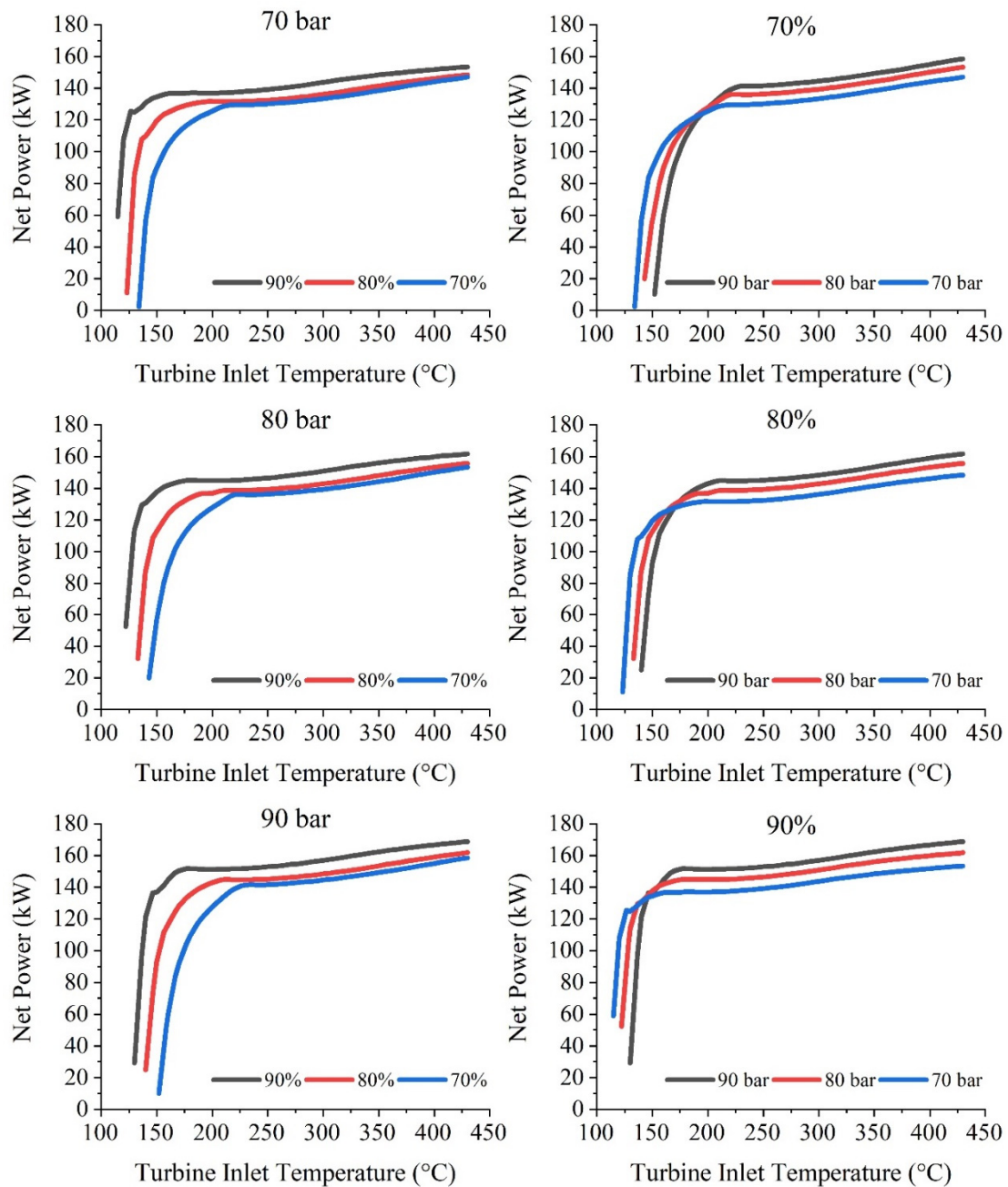


Figure 5. Effect of turbine inlet temperature for different pressures and mixing ratio of working fluid on net power of the Kalina Cycle.

Table 7. Exergy destruction of components of Kalina Cycle and Organic Rankine Cycle.

Cycle	Component	Exergy Inlet (kW)	Exergy Outlet (kW)	Exergy Destruction (kW)	Exergy Efficiency (%)
Kalina	Pump	77.19	76.14	1.05	98.64
	L HEX	506.50	500.45	6.06	98.80
	Evaporator	491.59	421.89	69.70	85.82
	Separator	353.74	353.74	0.00	100.00
	Turbine	353.74	334.04	19.70	94.43
	H HEX	87.43	87.38	0.05	99.94
	Condenser	162.41	77.83	84.58	47.92

Table 7. Cont.

Cycle	Component	Exergy Inlet (kW)	Exergy Outlet (kW)	Exergy Destruction (kW)	Exergy Efficiency (%)
ORC R123	Pump	16.06	15.65	0.42	97.41
	Evaporator	166.34	142.45	23.89	85.64
	Preheater	128.07	127.84	0.23	99.82
	Superheater	175.13	92.24	82.88	52.67
	Turbine	61.73	58.36	3.37	94.53
	Condenser	24.75	15	9.74	60.63

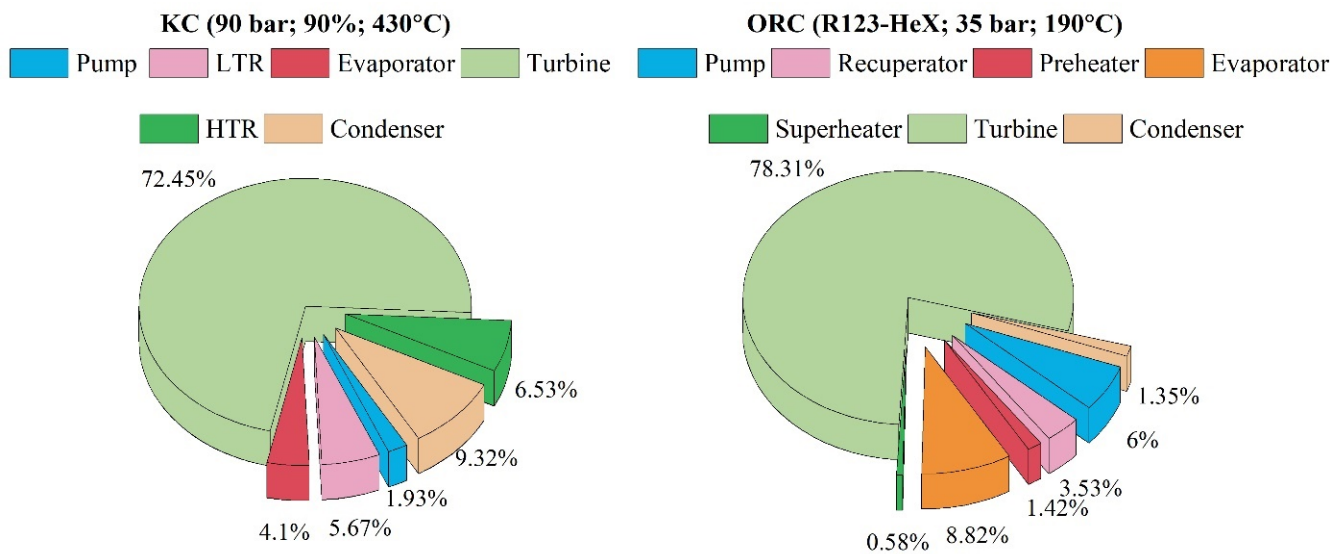


Figure 6. Exergy destruction separation in terms of components of KC and ORC.

When the cycle elements and performance parameters are considered together, it is necessary to carry out general exergy and energy calculations of the cycle in order to obtain a prediction of the general state of the whole system. To that end, the performance parameters, energy efficiency and exergy efficiency of the KC designed within the scope of this study were also calculated and given in Figures 7 and 8. The effect of the turbine inlet temperature, turbine inlet pressure and mixing ratio of the working fluid on the net thermal efficiency of the KC are shown in Figure 7.

The thermal efficiency of the KC increases with the increasing of the turbine inlet temperature and at a fixed inlet pressure of the turbine. The thermal efficiencies also increase with the ascending of the turbine inlet pressure. The net thermal efficiency increases very rapidly until it reaches 220 °C, which is the final temperature for the separation in the separator. At this turbine inlet temperature for the 90% mass fraction rate, the efficiency of the net thermal at 70 bar, 80 bar and 90 bar are 18.99%, 20.04% and 20.93% respectively. The maximum thermal efficiency of the best performing KC is 23.30% at the 90% ratio, 430 °C and 90 bar. The effect of the turbine inlet temperature and mixing ratio of the working fluid on the exergy efficiency of the KC are shown in Figure 8.

The exergy efficiency of the KC increases with the increasing of the turbine inlet temperature at varying turbine inlet pressures. The optimal cycle is obtained at 430 °C and 90 bar and the exergy efficiency is calculated as 50.20%.

The KC's low mass fraction rate and turbine inlet temperature values for every pressure tested are inefficient, according to the exergy and thermal efficiency results. At a constant temperature and pressure, the rise in the mass fraction ratio considerably improves both types of efficiencies.

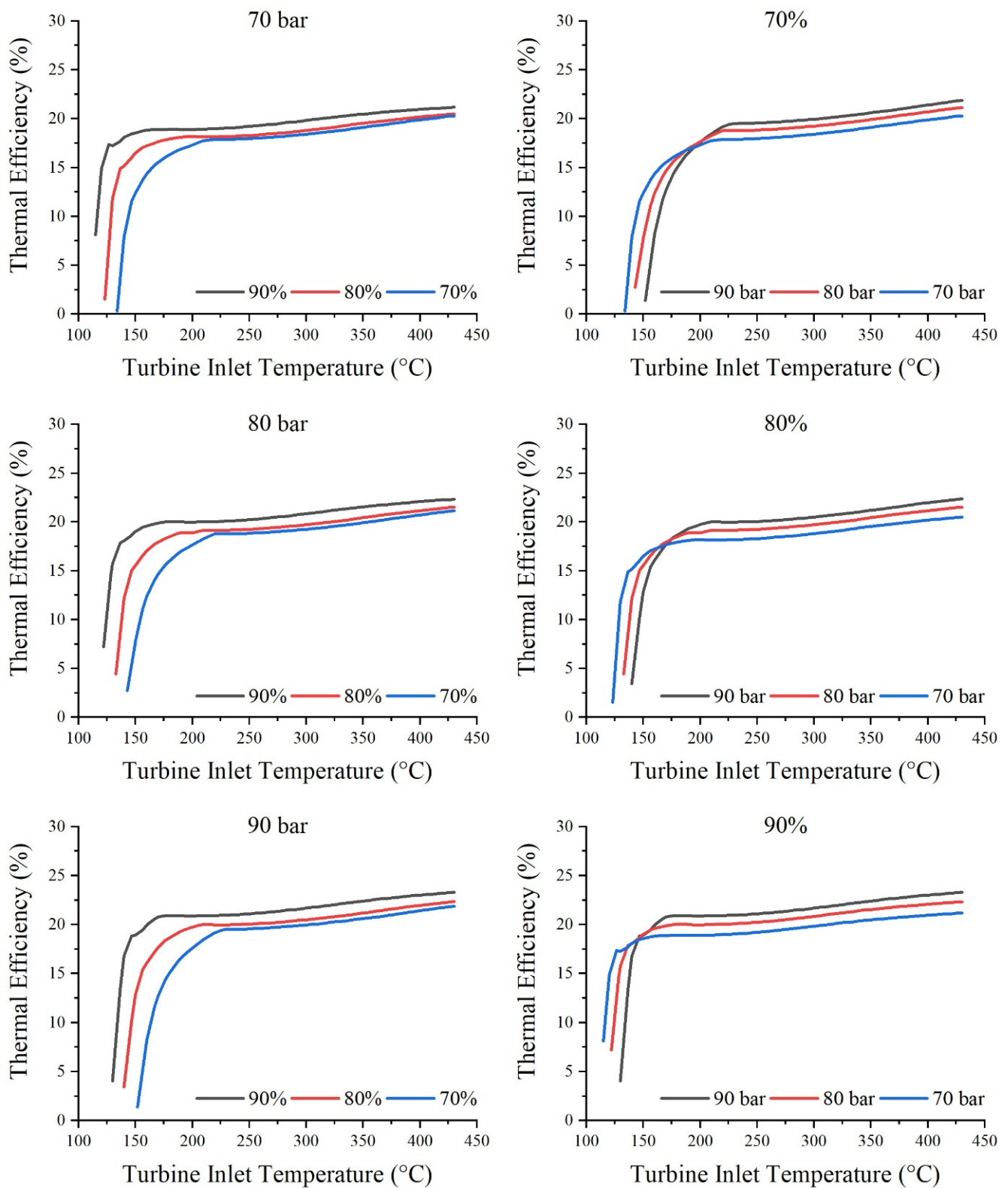


Figure 7. Effect of turbine inlet temperature, pressure and mixing ratio of working fluid on the net thermal efficiency of Kalina Cycle.

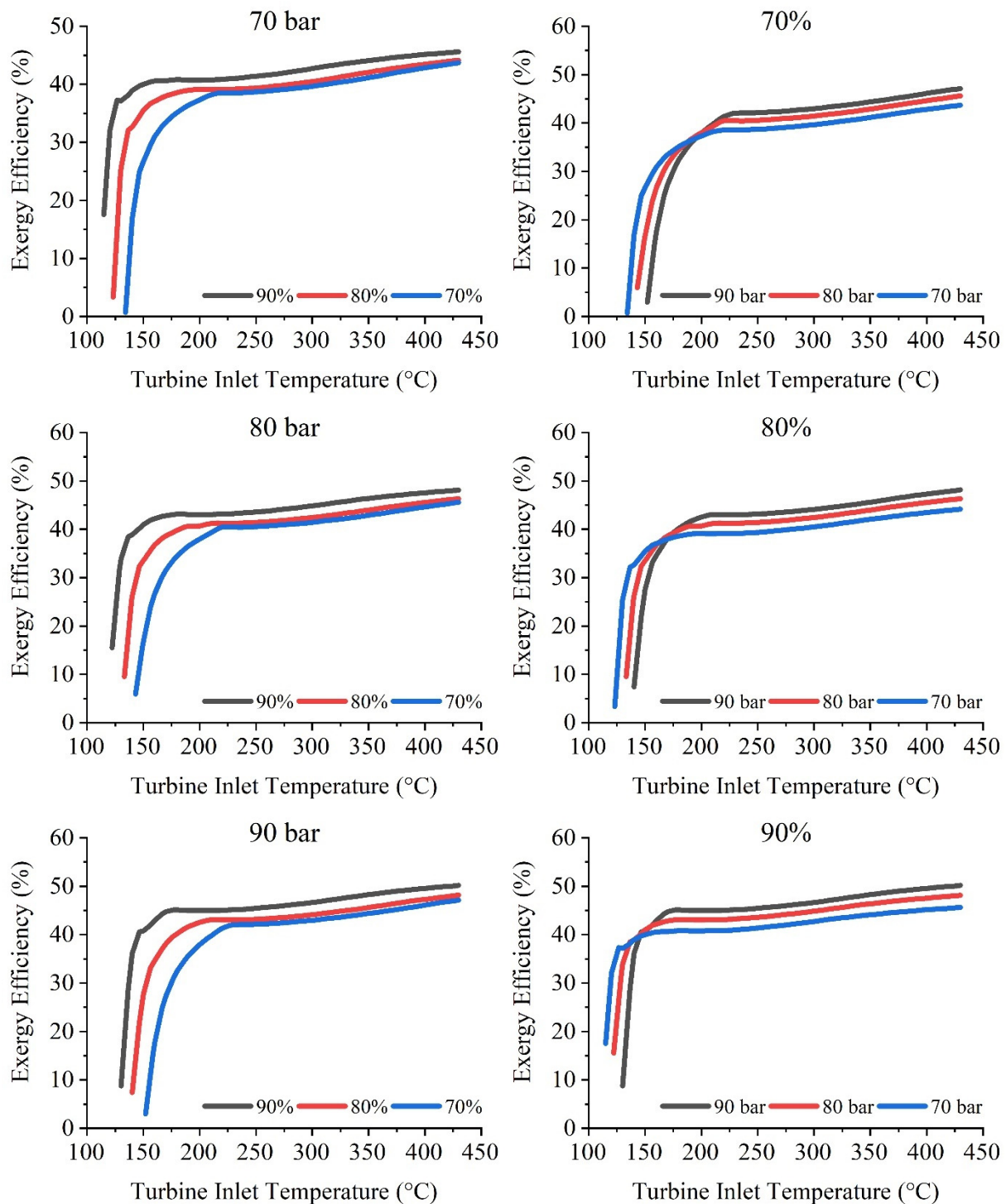


Figure 8. Effect of turbine inlet temperature, turbine inlet pressure and mixing ratio of working fluid on exergy efficiency of KC.

The results obtained in our study are consistent with the conclusions reached in similar studies in the literature. For example, in a study analysing KC cycles in a comparative manner, the maximum energy and exergy efficiencies were calculated as 24.99% and 71.77%, respectively, for the KC, in which a 90% ammonia–water mixture was used as the cycle fluid and a turbine inlet pressure of 100 bar [33]. In another study, the exergy efficiency of the KC was estimated to be 59.2% at the turbine inlet temperature of 152 °C and the turbine inlet pressure of 122 bar [34]. The authors claimed that at 150 °C TIT,

107.6 bar TIP and 0.949 ammonia–water combination, the KC had a thermal efficiency of 18.4% [35].

4.2. Optimization of ORC with Different Working Fluids with HEX and No HEX

The working liquid selection of an ORC is one of the most important steps in optimization studies. While there are numerous options with varying thermodynamic properties (critical pressure, etc.), liquid types (wet, dry, isentropic), environmental impacts and unit costs, three particular liquids, R236EA, R124 and R123, are selected and compared in this cycle design [36].

Before being merged into the main system, the net power output values of a single ORC were analysed. Furthermore, depending on the turbine input temperature, exergy and net thermal efficiencies were investigated at the point where the highest net power was generated. Pressure ranges of 10–33 bar were tested for the R236 fluid, while the range of 10 to 35 bar was tested for remaining fluids (R123 and R124). The inlet temperature of the turbine ranging between 60 °C and 140 °C was tested for R236 fluid and 60 °C and 190 °C for the fluids R123 and R124. From the equilibrium temperature of the working liquids, the least possible temperature of the cycle under stable pressure was detected [37].

Figure 9 shows the impact of TIT and pressure on the ORC's net power capacity. To speak about the chosen R236 fluid, the net power increases with increasing TIP but does not increase with the increasing turbine inlet temperature. The best performing cycle for the R236 fluid with HEX has the turbine inlet pressure and turbine inlet temperature values of 33 bar and 140 °C, respectively, and produces 35 kW at these points.

R124 fluid is also selected and tested for the cycle. For the no-HEX cycle, the net power decreases with the increasing turbine inlet temperature increase at constant pressure, and the net power increases with increasing turbine inlet pressure at a constant temperature. The best performing cycle has the turbine inlet pressure and temperature of 35 bar and 135 °C, respectively, and produces 38 kW.

The best performing ORC over all the cycles with the working fluid R123 with HEX has the optimum net power values of 42.34 kW at 190 °C, 35 bar. It can be seen that with the ascending turbine inlet temperature, the net power production increases but remains constant with the increasing turbine inlet temperature. Since the best performing cycle has working fluid of R123, it is also chosen for the combined KC and ORC.

Figure 10 displays the effect of the exergy efficiency of the ORC. As can be seen, for all the liquids chosen, the cycle exergy efficiency increases with higher turbine inlet pressure. In the cycle with the working fluid of 236 ea, the exergy efficiency remains constant at first until the turbine inlet pressure reaches 120 °C and then decreases slowly afterwards. For the cycle with fluid R124, the exergy efficiency decreases with higher turbine inlet pressure. In the case of R123, the exergy efficiency either does not change or slightly decreases with higher turbine inlet pressure. The best performing ORC–HEX system is obtained when R123 is used as a working fluid and the optimum exergy efficiency value is obtained at 190 °C, 35 bar and 35.29%.

Figure 11 shows the effect of TIT and TIP on the net thermal efficiency of the ORC. In the cycle with the working fluid 236 ea, the thermal efficiency remains constant until the turbine inlet pressure reaches 120 °C and starts decreasing afterwards. The thermal efficiency of the cycle with fluid R124 decreases with higher turbine inlet pressure, while the thermal efficiency of the cycle with R123 either does not change or slightly decreases with higher turbine inlet pressures. For the best performing ORC with HEX, the working fluid R123 has the optimum net thermal efficiency values at 190 °C turbine inlet temperature and 35 bar turbine inlet pressure is 21.73%.

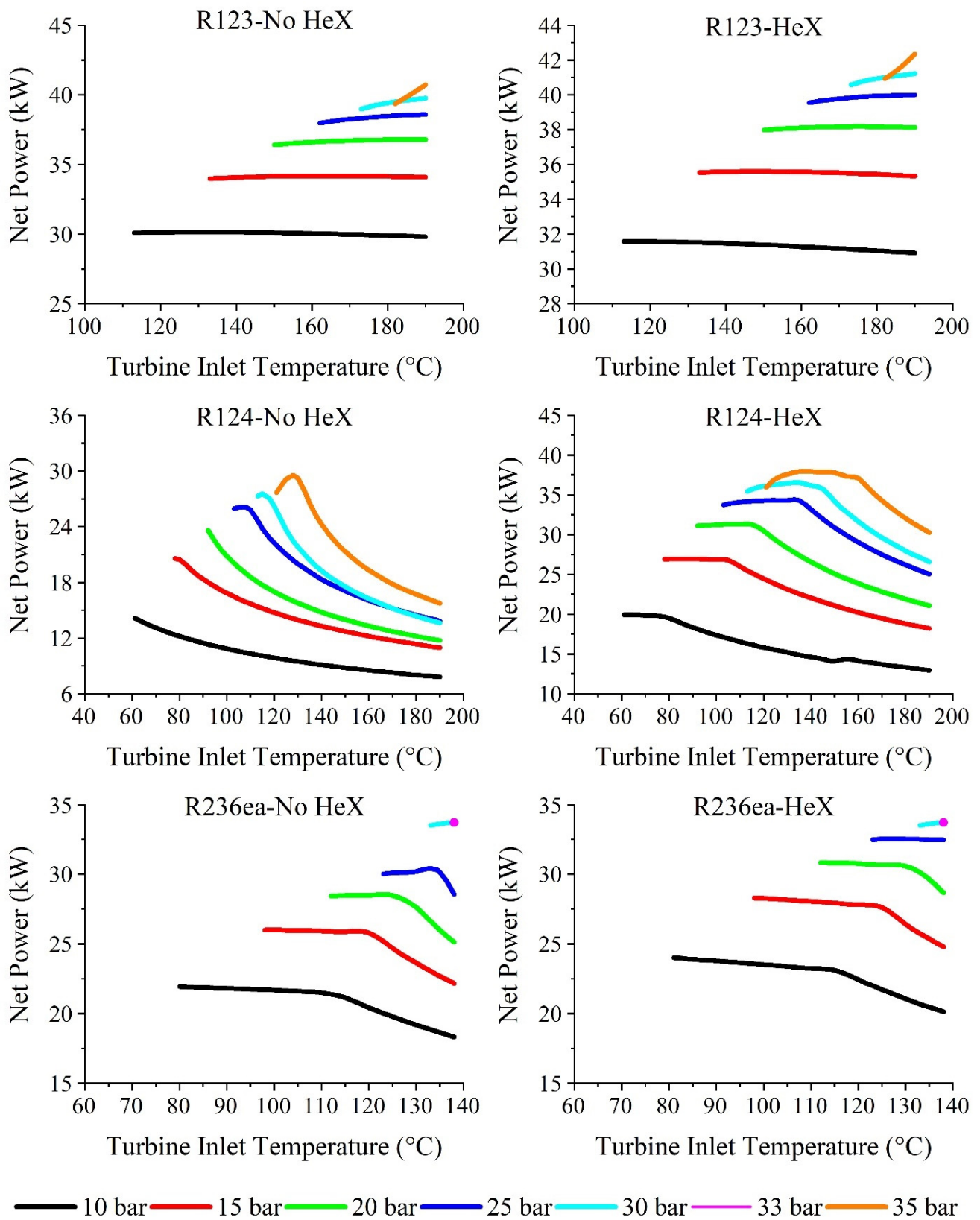


Figure 9. For various working fluids, the effect of TIT and TIP on net power of the ORC.

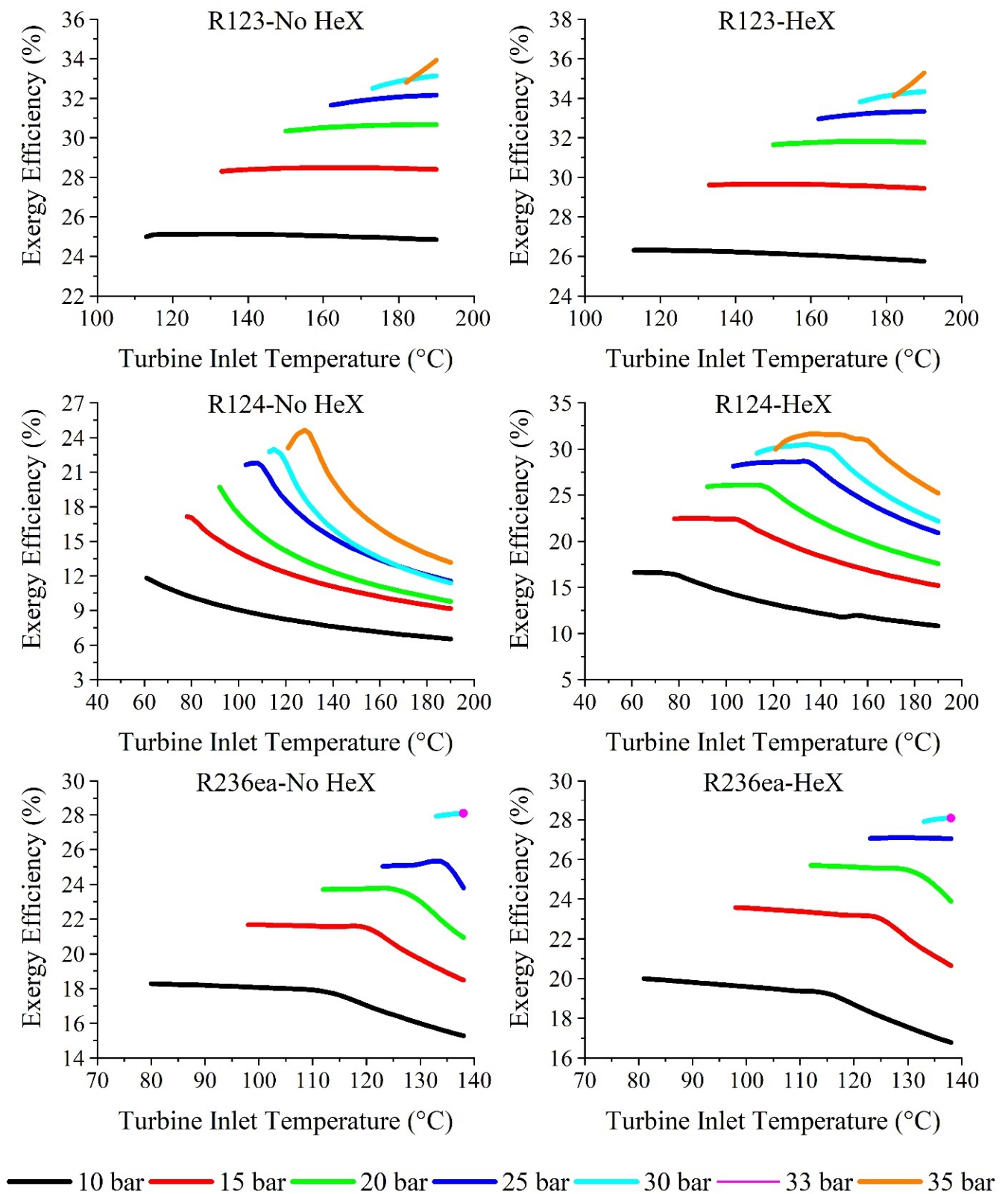


Figure 10. Effects of turbine inlet temperature and pressure on ORC exergy efficiency for various working fluids.

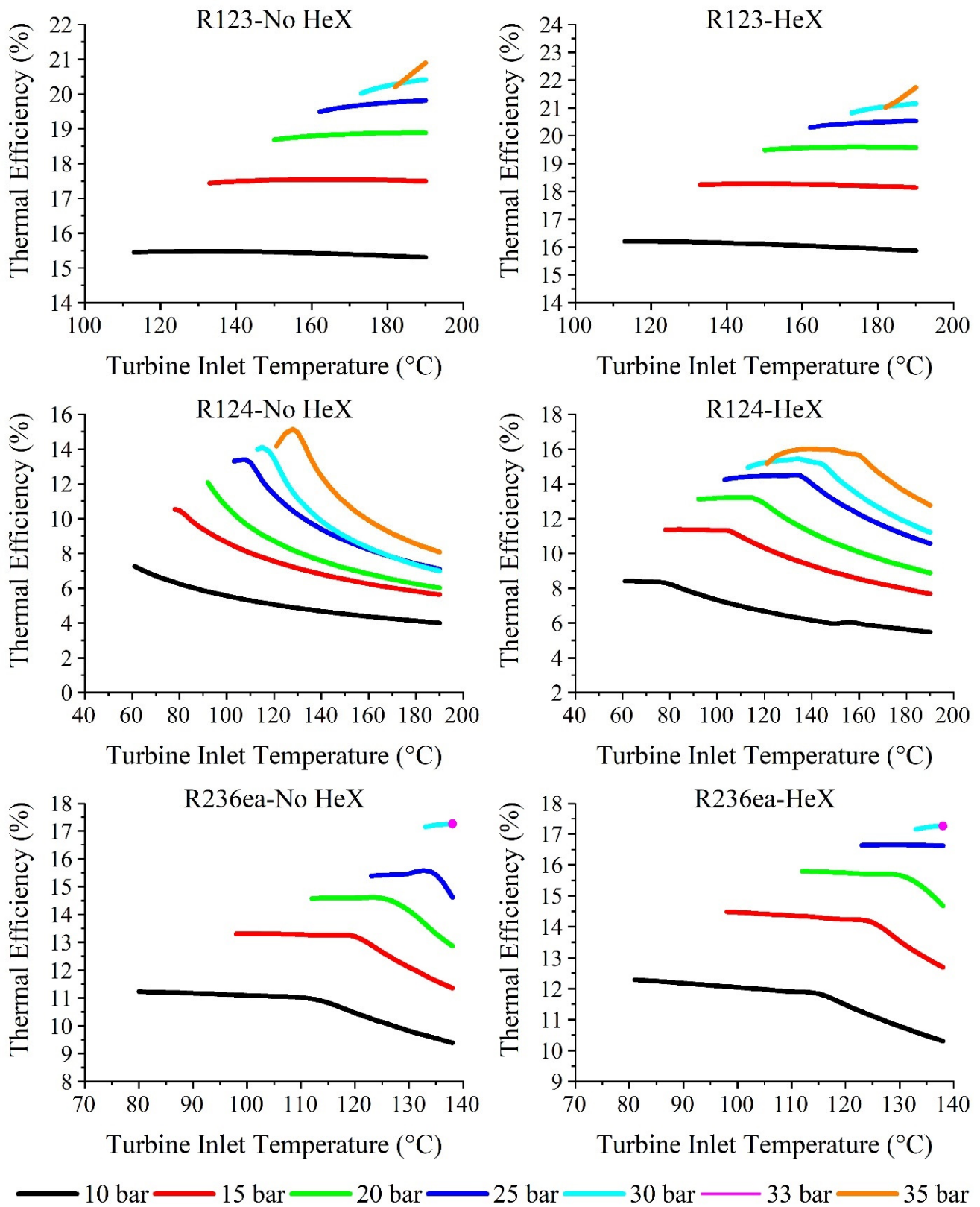


Figure 11. For various working fluids, the effect of turbine inlet temperature and pressure on the net thermal efficiency of the ORC.

In a study in which ORC cycles were analysed and compared, the overall highest net thermal and exergy efficiencies were found as 41.72% and 41.01%, respectively, at a value of 100 bar RC TIP and 480 °C RC TIT [38].

4.3. Result Comparison of Combined Best Performed KC and ORC with R123 Working Fluid

If the temperature of the depleted gas exit is too low to employ traditional methods, medium and low temperature power cycles like the KC from a new generation are acceptable for using the depleted gas vented into the air [39]. The KC is then integrated with the RC to generate as much energy as feasible from the combined process. In Figure 12, the change of performance parameters is shown for the combined KC with turbine inlet temperatures of 430 °C and 90 bar with the mass fraction of 90% and ORC with the most efficient fluid R123.

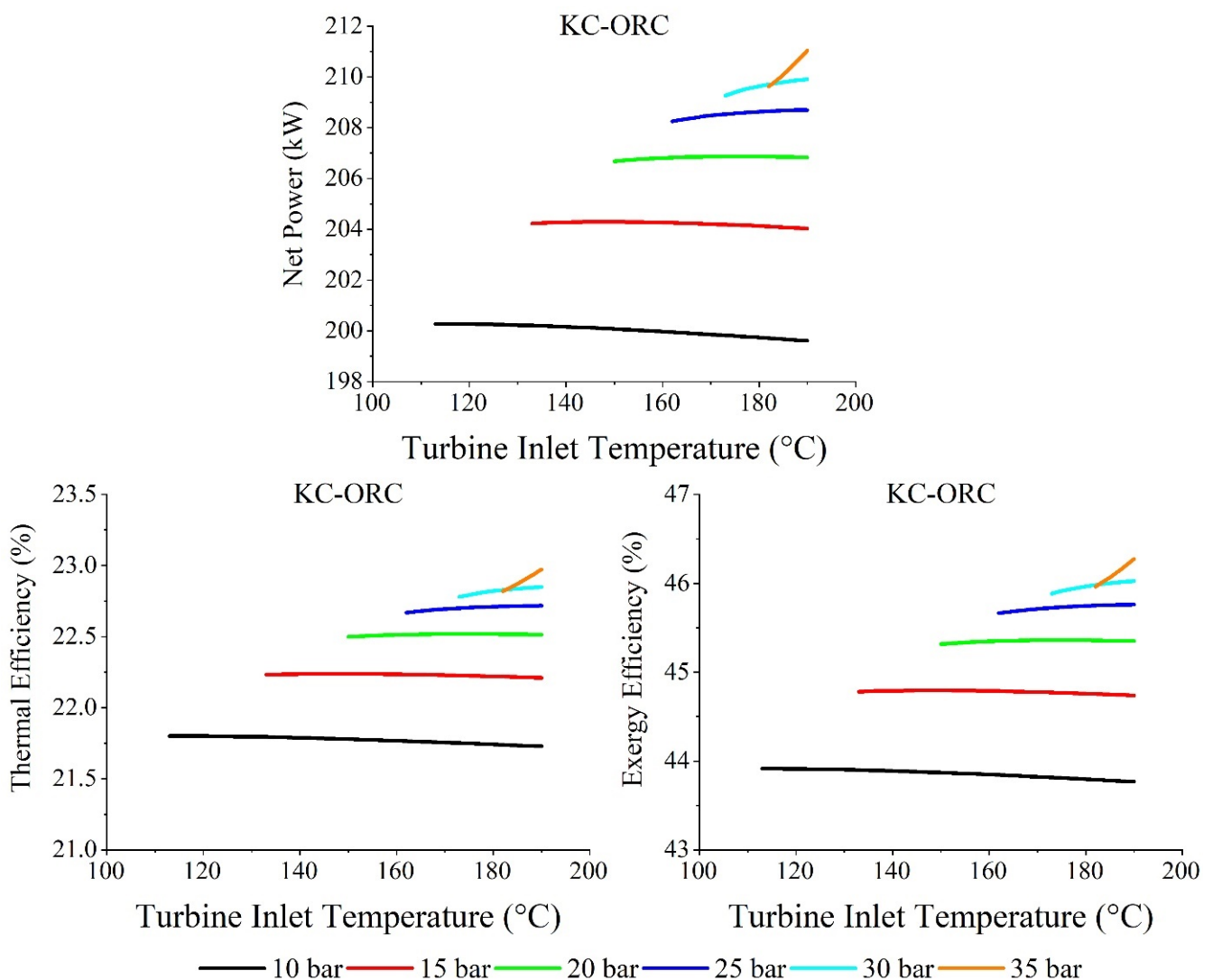


Figure 12. The sequence of TIT and TIP on net power, exergy efficiency and energy efficiency of combined KC and ORC.

The designed cycle has a pressure varying from 10 bar to 35 bar, while the temperature of the turbine inlet varies between 100 °C and 190 °C. With the working fluid of R123, the best performed hybrid KC and ORC has the maximum thermal efficiency and energy efficiency and net power values at 190 °C, 35 bar at 26.50% and 52.83% at 211.03 kW, respectively.

In Figure 13, the jacket water added system (cogeneration) is shown in terms of net thermal efficiency and exergy efficiency.

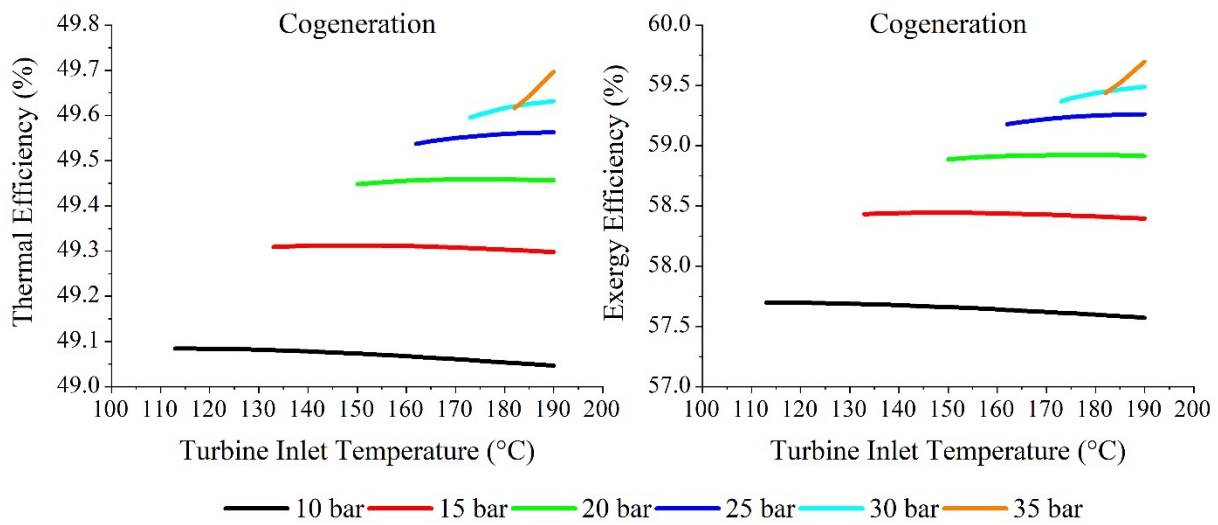


Figure 13. The effect of turbine inlet temperature and pressure on the combined KC, ORC, and Jacket Water Heating’s (Cogeneration) net thermal efficiency and exergy efficiency.

If jacket water heating is added to the system, the energy and exergy efficiencies increase, as shown in Figure 13. The maximum thermal efficiency is found to be 49.74% and exergy efficiency is found to be 59.75% at 35 bar TIP and 190 °C TIT of the ORC.

4.4. Economical Result

Nowadays, scientific research is attempting to develop an environmentally friendly and economically feasible system in addition to determining the capacity of a designed system or enhancing the overall efficiencies of a system [40,41]. The economic feasibility analysis of the KC and ORC is also included in this study to demonstrate the economic aspects and benefits of the planned system.

As a first step, the purchased equipment cost (PEC) for the RC and KC was determined using the costs shown in Figure 14 and Table 8. The compensation period of all ORC, KC and ORC–KC was then evaluated, considering the yearly rate of interest, yearly working hours, time of life and sales price of electricity. Expenses of the RC and KC’s purchased equipment are shown in Table 8 while their distribution is shown in Figure 14.

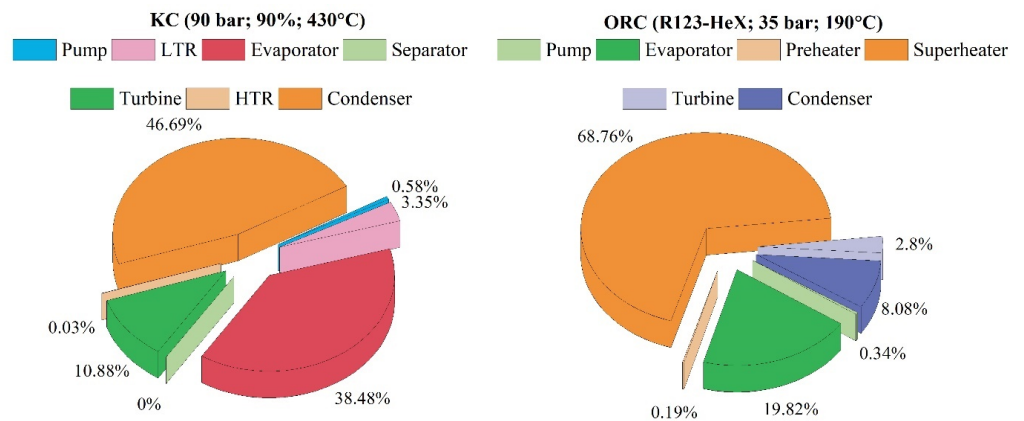


Figure 14. Purchased equipment cost of ORC and KC in percent.

Table 8. ORC and KC Equipment costs [26].

Part	ORC (PEC)-DOLLAR	Part	KC (PEC)-DOLLAR
Pump	\$6572.92	Pump	\$4352.45
Recuperator	\$3870.87	LTR	\$12,763.80
Preheater	\$1556.91	HTR	\$14,705.62
Evaporator	\$9663.83	Evaporator	\$9239.20
Superheater	\$630.67	Turbine	\$163,151.63
Turbine	\$85,827.57	Condenser	\$20,993.74
Condenser	\$1478.87		

The KC's and ORC's investment cost evaluations and payback year calculations were carried out by taking into account the component investment costs. Table 9 shows the payback period calculation for the combined KC and ORC system, which is found to be 4.2 years.

Table 9. Combined Cycle payback period [26].

n (Plantlife)	N (Annual Operation Time)	i (Interest Rate)	Acceptations-Maximum Point				Purchased Equipment Cost (PEC)	OVERALL NET POWER	Payback Period
			Operation and Maintenance Factor	Electrical Sale Value	Maintenance Operation Cost				
Year	Hour	-	-	\$/kWh	\$	\$	kW	Years	
15 year	7680 year/h	0.12	mf = 1.06			KALINA + ORC	KALINA + ORC		
15.00	7680.00	0.15	1.060	0.07	2008.85	334,807.63	211.04	4.29	

The results of the economic evaluation are consistent with the findings of similar studies in the literature. For example, in an economic analysis of the KC as part of a combined power system, the KC's payback period was found to be around three years, while the cost of investment was decreased to 1.000 \$ per kW hour after conducting extensive research and analysis [42]. In another study, it was discovered that the payback period and cost of the total investment of the KC were 5.8 years and 1300 \$ per kW hour, respectively [43–48].

5. Conclusions

The main limitation of this study is the exhaust gas of the biogas engine, which is 450 °C cooled to 120 °C while transferring its energy to electricity in the Kalina Cycle (Table 1). In these circumstances, in a single KC for 90 bar TIP and 430 °C TIT with a mass fraction of 90%, the maximum net power of 168.69 kW can be generated. For the single Organic Rankine Cycle with working fluid R123, the maximum power of 42.34 kW can be generated at 190 °C TIT and 35 bar TIP. It has been observed that approximately 211.03 kW of net power can be obtained if the waste energy of the exhaust gas discharged into the atmosphere without being used in the current situation is recovered using the combined KC and ORC cycles. In the single KC for 90 bar TIP and 430 °C TITs with the mass fraction of 90%, thermal efficiency and exergy efficiencies were 23.30% and 50.20% in order. Moreover, the energy efficiency and exergy efficiency of the combined structure have been calculated as 26.50% and 52.83%, in order.

Not only is the waste heat gas of the motor recovered, but the heat of the jacket water of the engine is also recovered by using two heat exchangers in the system. The first heat exchanger cools down the jacket water from 86 °C to 80 °C while preheating the KC working fluid. The second heat exchanger is used to cool down from 80 °C to 70 °C while preheating the cool water with a mass flow rate of 3.17 kg/s. The cooled water preheated by the jacket water enters another heat exchanger to heat up to 70 °C by the exhaust gas leaving from the KC at 120 °C. The maximum thermal efficiency of the cogeneration is

found to be 49.74% and exergy efficiency is found to be 59.75% at 35 bar TIP and 190 °C TIT of ORC.

First, with the equations of the cost given, the obtained hardware costs of the RC and KC were found. After that, by not ignoring the annual loan expense, yearly working time, time of life and energy cost, the payback duration of all the RC, KC and the combined cycle was found. The payback period of the coordinates of the combined cycle was estimated as 4.2 years, which is very feasible to invest in such an efficient technology.

One of the key but overlooked aspects of sustainability is identifying possible impacts of systems and processes on people (so-called social sustainability). The economic growth that comes from the conversion of underutilized sources through waste heat recovery systems can only be sustained if these practices support profitability without negatively affecting social and environmental determinants of health. Hence, future research should focus on extending the economic cost-benefit analysis of waste heat recovery systems in a way to account for all costs and benefits including social and environmental effects. Further development of such social cost-benefit analysis approaches to assess whether the undesired effects outweigh the benefits gained in waste heat recovery will help in the pursuit of a more sustainable energy future. In addition, future research in this field should focus on increasing the efficiency of not only using the energy of exhaust gas but also using the energy of lubricating oil of the biogas engine.

Author Contributions: A.K. and C.Ö. formed the main theme of the article and carried out data collection, ideology and optimization studies; A.K. and C.Ö. contributing equal to the final distribution of the research investigation to compose the article; A.K. contributed to the review and editing of the article. All authors have read and agreed to the published version of the manuscript.

Funding: This research has received no external funding.

Institutional Review Board Statement: Not applicable.

Informed Consent Statement: Not applicable.

Data Availability Statement: Not applicable.

Conflicts of Interest: The authors declare no conflict of interest.

Nomenclature

A	area (m ²)
ASHRAE	American society of heating, refrigerating and air-conditioning engineers
CF	capacity factor
CHP	combined heat and power
CRF	capital recovery factor
EPC	electrical performance capacity (%)
\dot{E}	exergy flow (kW)
GT	gas turbine
GWP	global warming potential
h	enthalpy (kJ/kg)
i	interest rate (%)
HEX	heat exchanger
HTR	high temperature recuperator
KC	Kalina Cycle
LHV	low heating value (kJ/kg)
LMTD	logarithmic mean temperature difference
LTR	low temperature recuperator
MEP	biogas engine electrical power (kW)
MPC	biogas engine mechanical performance capability (%)
\dot{m}	mass flow rate (kg/s)
N	lifetime (year)

NOE	number of engines
n	annual operation time (hour)
ODP	ozone depletion potential
ORC	Organic Rankine Cycle
\dot{Q}	heat flow (kW)
P	pressure (bar)
PB	payback period (year)
PEC	purchased equipment cost (\$)
RC	Rankine cycle
s	entropy (kJ/kgK)
T_0	ambient temperature (°C)
T	temperature (°C)
TIT	turbine inlet temperature (°C)
TPC	thermal performance capacity
TIP	turbine inlet pressure (bar)
U	heat transfer coefficient (kW/m ² K)
\dot{W}	power (kW)
X	ammonia-water mass fraction ratio (%)
Greek Letters	
ψ	specific exergy (kJ/kg)
ε	exergetic efficiency (%)
ϵ	burner effectiveness (%)
η	thermal efficiency (%)
ϕ	maintenance factor

References

- Dejfors, C.; Svedberg, G. Second law analysis of ammonia-water power cycle for direct-fired cogeneration application. *Int. J. Thermodyn.* **1999**, *2*, 125–131.
- Maizza, V.; Maizza, A. Unconventional working fluids in organic Rankine-cycles for waste energy recovery systems. *Appl. Therm. Eng.* **2001**, *21*, 381–390. [[CrossRef](#)]
- Little, A.B.; Garimella, S. Comparative assessment of alternative cycles for waste heat recovery and upgrade. *Energy* **2011**, *36*, 4492–4504. [[CrossRef](#)]
- Kalina, A.; Leibowitz, H. *System Design and Experimental Development of the Kalina Cycle Technology*; Energy Systems Laboratory: Bryan, TX, USA, 1987.
- He, M.; Zhang, X.; Zeng, K.; Gao, K. A combined thermodynamic cycle used for waste heat recovery of internal combustion engine. *Energy* **2011**, *36*, 6821–6829. [[CrossRef](#)]
- Mehrpooya, M.; Ghorbani, B.; Hosseini, S.S. Developing and exergetic performance assessment of biogas upgrading process driven by flat plate solar collectors coupled with Kalina power cycle. *Energy Convers. Manag.* **2019**, *181*, 398–413. [[CrossRef](#)]
- Tian, H.; Shu, G.; Wei, H.; Liang, X.; Liu, L. Fluids and parameters optimization for the organic Rankine cycles (ORCs) used in exhaust heat recovery of Internal Combustion Engine (ICE). *Energy* **2012**, *47*, 125–136. [[CrossRef](#)]
- Liu, B.-T.; Chien, K.-H.; Wang, C.-C. Effect of working fluids on organic Rankine cycle for waste heat recovery. *Energy* **2004**, *29*, 1207–1217. [[CrossRef](#)]
- Nižetić, S.; Papadopoulos, A. *The Role of Exergy in Energy and the Environment*; Springer: Berlin/Heidelberg, Germany, 2018.
- Köse, Ö.; Koç, Y.; Yağlı, H. Performance improvement of the bottoming steam Rankine cycle (SRC) and organic Rankine cycle (ORC) systems for a triple combined system using gas turbine (GT) as topping cycle. *Energy Convers. Manag.* **2020**, *211*, 112745. [[CrossRef](#)]
- Yağlı, H.; Koç, Y.; Köse, Ö.; Koç, A.; Yumrutaş, R. Optimisation of simple and regenerative organic Rankine cycles using jacket water of an internal combustion engine fuelled with biogas produced from agricultural waste. *Process Saf. Environ. Prot.* **2021**, *155*, 17–31. [[CrossRef](#)]
- Koç, Y.; Yağlı, H.; Koç, A. Exergy analysis and performance improvement of a subcritical/supercritical organic rankine cycle (ORC) for exhaust gas waste heat recovery in a biogas fuelled combined heat and power (CHP) engine through the use of regeneration. *Energies* **2019**, *12*, 575. [[CrossRef](#)]
- Koç, Y.; Yağlı, H.; Kalay, I. Energy, exergy, and parametric analysis of simple and recuperative organic Rankine cycles using a gas turbine-based combined cycle. *J. Energy Eng.* **2020**, *146*, 04020041. [[CrossRef](#)]
- Mert, İ.; Bilgic, H.H.; Yağlı, H.; Koç, Y. Deep neural network approach to estimation of power production for an organic Rankine cycle system. *J. Braz. Soc. Mech. Sci. Eng.* **2020**, *42*, 1–16. [[CrossRef](#)]
- Koc, Y.; Yagli, H.; Ozdes, E.O.; Baltacioglu, E.; Koc, A. Thermodynamic analysis of solid waste and energy consumption to reduce the effects of an electric arc furnace on the environment. *Int. J. Glob. Warm.* **2019**, *19*, 308–323. [[CrossRef](#)]

16. Koc, Y.; Aksar, M.; Yagli, H. First and second law-based thermal optimisation of the Kalina cycle integrated into an existing burner-based cogeneration system using waste chips as fuel. *Int. J. Exergy* **2020**, *33*, 165–182. [[CrossRef](#)]
17. Yağlı, H. Examining the receiver heat loss, parametric optimization and exergy analysis of a solar power tower (SPT) system. *Energy Sources Part A Recovery Util. Environ. Eff.* **2020**, *42*, 2155–2180. [[CrossRef](#)]
18. Lee, H.Y.; Kim, K.H. Energy and exergy analyses of a combined power cycle using the organic rankine cycle and the cold energy of liquefied natural gas. *Entropy* **2015**, *17*, 6412–6432. [[CrossRef](#)]
19. Akbari, M.; Mahmoudi, S.; Yari, M.; Rosen, M.A. Energy and exergy analyses of a new combined cycle for producing electricity and desalinated water using geothermal energy. *Sustainability* **2014**, *6*, 1796–1820. [[CrossRef](#)]
20. Li, S.; Dai, Y. Thermo-economic comparison of Kalina and CO₂ transcritical power cycle for low temperature geothermal sources in China. *Appl. Therm. Eng.* **2014**, *70*, 139–152. [[CrossRef](#)]
21. Seckin, C. Thermodynamic analysis of a combined power/refrigeration cycle: Combination of Kalina cycle and ejector refrigeration cycle. *Energy Convers. Manag.* **2018**, *157*, 631–643. [[CrossRef](#)]
22. Yağlı, H.; Koç, Y.; Kalay, H. Optimisation and exergy analysis of an organic Rankine cycle (ORC) used as a bottoming cycle in a cogeneration system producing steam and power. *Sustain. Energy Technol. Assess.* **2021**, *44*, 100985. [[CrossRef](#)]
23. Kim, Y.M.; Sohn, J.L.; Yoon, E.S. Supercritical CO₂ Rankine cycles for waste heat recovery from gas turbine. *Energy* **2017**, *118*, 893–905. [[CrossRef](#)]
24. Meng, F.; Wang, E.; Zhang, B.; Zhang, F.; Zhao, C. Thermo-economic analysis of transcritical CO₂ power cycle and comparison with Kalina cycle and ORC for a low-temperature heat source. *Energy Convers. Manag.* **2019**, *195*, 1295–1308. [[CrossRef](#)]
25. Chen, Y.; Guo, Z.; Wu, J.; Zhang, Z.; Hua, J. Energy and exergy analysis of integrated system of ammonia–water Kalina–Rankine cycle. *Energy* **2015**, *90*, 2028–2037. [[CrossRef](#)]
26. Yağlı, H.; Koç, Y.; Koç, A.; Görgülü, A.; Tandiroğlu, A. Parametric optimization and exergetic analysis comparison of subcritical and supercritical organic Rankine cycle (ORC) for biogas fuelled combined heat and power (CHP) engine exhaust gas waste heat. *Energy* **2016**, *111*, 923–932. [[CrossRef](#)]
27. Köse, Ö.; Koç, Y.; Yağlı, H. Energy, exergy, economy and environmental (4E) analysis and optimization of single, dual and triple configurations of the power systems: Rankine Cycle/Kalina Cycle, driven by a gas turbine. *Energy Convers. Manag.* **2021**, *227*, 113604. [[CrossRef](#)]
28. Mohammadkhani, F.; Shokati, N.; Mahmoudi, S.; Yari, M.; Rosen, M. Exergoeconomic assessment and parametric study of a Gas Turbine-Modular Helium Reactor combined with two Organic Rankine Cycles. *Energy* **2014**, *65*, 533–543. [[CrossRef](#)]
29. Liu, Z.; He, T. Exergoeconomic analysis and optimization of a Gas Turbine-Modular Helium Reactor with new organic Rankine cycle for efficient design and operation. *Energy Convers. Manag.* **2020**, *204*, 112311. [[CrossRef](#)]
30. Pourpasha, H.; Mohammadfam, Y.; Khani, L.; Mohammadpourfard, M.; Heris, S.Z. Thermodynamic and thermoeconomic analyses of a new dual-loop organic Rankine–Generator absorber heat exchanger power and cooling cogeneration system. *Energy Convers. Manag.* **2020**, *224*, 113356. [[CrossRef](#)]
31. Özahi, E.; Tozlu, A.; Abuşoğlu, A. Thermoeconomic multi-objective optimization of an organic Rankine cycle (ORC) adapted to an existing solid waste power plant. *Energy Convers. Manag.* **2018**, *168*, 308–319. [[CrossRef](#)]
32. Mamaghani, A.H.; Najafi, B.; Shirazi, A.; Rinaldi, F. 4E analysis and multi-objective optimization of an integrated MCFC (molten carbonate fuel cell) and ORC (organic Rankine cycle) system. *Energy* **2015**, *82*, 650–663. [[CrossRef](#)]
33. Kim, K.H.; Han, C.H.; Kim, K. Comparative exergy analysis of ammonia–water based Rankine cycles with and without regeneration. *Int. J. Exergy* **2013**, *12*, 344–361. [[CrossRef](#)]
34. Dai, Y.; Wang, J.; Gao, L. Parametric optimization and comparative study of organic Rankine cycle (ORC) for low grade waste heat recovery. *Energy Convers. Manag.* **2009**, *50*, 576–582. [[CrossRef](#)]
35. Sadaghiani, M.S.; Ahmadi, M.; Mehrpooya, M.; Pourfayaz, F.; Feidt, M. Process development and thermodynamic analysis of a novel power generation plant driven by geothermal energy with liquefied natural gas as its heat sink. *Appl. Therm. Eng.* **2018**, *133*, 645–658. [[CrossRef](#)]
36. Mago, P.J.; Chamra, L.M.; Srinivasan, K.; Somayaji, C. An examination of regenerative organic Rankine cycles using dry fluids. *Appl. Therm. Eng.* **2008**, *28*, 998–1007. [[CrossRef](#)]
37. Yari, M.; Mehr, A.; Zare, V.; Mahmoudi, S.; Rosen, M. Exergoeconomic comparison of TLC (trilateral Rankine cycle), ORC (organic Rankine cycle) and Kalina cycle using a low grade heat source. *Energy* **2015**, *83*, 712–722. [[CrossRef](#)]
38. Wang, J.; Sun, Z.; Dai, Y.; Ma, S. Parametric optimization design for supercritical CO₂ power cycle using genetic algorithm and artificial neural network. *Appl. Energy* **2010**, *87*, 1317–1324. [[CrossRef](#)]
39. Sireesha, M.; Jagadeesh Babu, V.; Kranthi Kiran, A.S.; Ramakrishna, S. A review on carbon nanotubes in biosensor devices and their applications in medicine. *Nanocomposites* **2018**, *4*, 36–57. [[CrossRef](#)]
40. Song, J.; Li, X.; Wang, K.; Markides, C.N. Parametric optimisation of a combined supercritical CO₂ (S-CO₂) cycle and organic Rankine cycle (ORC) system for internal combustion engine (ICE) waste-heat recovery. *Energy Convers. Manag.* **2020**, *218*, 112999. [[CrossRef](#)]
41. Rashidi, J.; Ifaei, P.; Esfahani, I.J.; Ataei, A.; Yoo, C.K. Thermodynamic and economic studies of two new high efficient power-cooling cogeneration systems based on Kalina and absorption refrigeration cycles. *Energy Convers. Manag.* **2016**, *127*, 170–186. [[CrossRef](#)]

42. Ogriseck, S. Integration of Kalina cycle in a combined heat and power plant, a case study. *Appl. Therm. Eng.* **2009**, *29*, 2843–2848. [[CrossRef](#)]
43. Coskun, A.; Bolatturk, A.; Kanoglu, M. Thermodynamic and economic analysis and optimization of power cycles for a medium temperature geothermal resource. *Energy Convers. Manag.* **2014**, *78*, 39–49. [[CrossRef](#)]
44. Kim, K.H.; Han, C.H.; Kim, K. Effects of ammonia concentration on the thermodynamic performances of ammonia–water based power cycles. *Thermochim. Acta* **2012**, *530*, 7–16. [[CrossRef](#)]
45. Singh, O.K.; Kaushik, S. Energy and exergy analysis and optimization of Kalina cycle coupled with a coal fired steam power plant. *Appl. Therm. Eng.* **2013**, *51*, 787–800. [[CrossRef](#)]
46. Wang, J.; Dai, Y.; Zhang, T.; Ma, S. Parametric analysis for a new combined power and ejector–absorption refrigeration cycle. *Energy* **2009**, *34*, 1587–1593. [[CrossRef](#)]
47. Ashouri, M.; Vandani, A.M.K.; Mehrpooya, M.; Ahmadi, M.H.; Abdollahpour, A. Techno-economic assessment of a Kalina cycle driven by a parabolic Trough solar collector. *Energy Convers. Manag.* **2015**, *105*, 1328–1339. [[CrossRef](#)]
48. Cao, L.; Wang, J.; Dai, Y. Thermodynamic analysis of a biomass-fired Kalina cycle with regenerative heater. *Energy* **2014**, *77*, 760–770. [[CrossRef](#)]